Enantiomeric excess dependence of the phase diagram of antiferroelectric liquid crystals

E. Gorecka,[1,2] D. Pociecha,[1] M. Čepič,[3] B. Žekš,[3] and R. Dabrowski[4]
[1]*Chemistry Department, Warsaw University, Al. Zwirki i Wigury 101, 02-089 Warsaw, Poland*
[2]*Department of Microelectronics and Nanoscience, Chalmers University of Technology, S-41296 Göteborg, Sweden*
[3]*Jožef Stefan Institute, Jamova 39, 1000 Ljubljana, Slovenia*
[4]*Institute of Chemistry, Military University of Technology, 00-908 Warsaw, Poland*
(Received 13 September 2001; revised manuscript received 5 April 2002; published 13 June 2002)

The phase diagram of the prototype antiferroelectric liquid crystal 4-(1-methylheptyloxycarbonyl)phenyl-4′-octyloxybiphengl-4-carboxylate (MHPOBC) in dependence of enantiomeric excess was measured. It was shown that the Sm-C^*_β phase in very pure samples is the Sm-C^*_{FI2} phase with a four-layer structure, and only after small racemization it transforms into the ferroelectric Sm-C^* phase. The phase diagram was theoretically explained by taking into account longer range bilinear and short range biquadratic interlayer interactions, that lead to the distorted clock structures and first-order transitions between them.

DOI: 10.1103/PhysRevE.65.061703 PACS number(s): 61.30.Cz

In some systems chiral properties can be transferred from a molecular to a macroscopic level. The best examples of such systems are liquid crystals that form chiral phases (cholesteric, blue, twist grain boundary, or polar smectic phases), if built of chiral molecules. The variation of the enantiomeric excess influences macroscopic properties of these phases such as the period of the modulation and the phase transition temperature or it can even change the phase sequence. The striking example of the last phenomenon are antiferroelectric liquid crystals where some phases disappear with racemization [1]. For high optical purity 4-(1-methylheptyloxycarbonyl)phenyl-4′-octyloxybiphengl-4-carboxylate (MHPOBC) compound, the prototype antiferroelectric material, the sequence of tilted phases Sm-$C^*_\alpha \leftrightarrow$ Sm-$C^*_\beta \leftrightarrow$ Sm-$C^*_\gamma \leftrightarrow$ Sm-C^*_A was reported with decreasing temperature [2]. In the partially racemized sample only two of these phases, Sm-C^*_β and Sm-C^*_A, remained. The Sm-C^*_A phase is the phase with the antiferroelectric properties and antiparallel tilts in neighboring layers, i.e., anticlinic phase. The Sm-C^*_β phase has been recognized as the ferroelectric synclinic Sm-C^* phase. Almost ten years later structures of the other subphases have been found by resonant x-ray scattering in a different compound 4-[(4-{[1(*)-methyl]heptycarboxy} phenyl)carboxy]phenyl-4′-decyloxy-1-benzencarbaticate (10 OTBBB1M7) [3]. In this compound the phase sequence with decreasing temperature is the Sm-C^*_α phase with the periodical modulation of a tilt direction and with five- or more, in general incommensurate, number of layers, the Sm-C^*_{FI2} phase with four-layer modulation, the Sm-C^*_{FI1} phase with three-layer modulation, and the Sm-C^*_A phase with two-layer structure. The Sm-C^*_{FI1} phase in the 10OTBBB1M7 compound corresponds to the Sm-C^*_γ phase in MHPOBC material. So far theoretical considerations failed to account for the correct phase sequences in dependence of enantiomeric excess as well as experimentally consistent structures of some phases.

In this paper we present the complete phase diagram for the antiferroelectric system MHPOBC with respect to the enantiomeric excess. We show that the synclinic Sm-C^* phase transforms into the Sm-C^*_{FI2} phase upon increasing optical purity. The result solves the long known controversy why the smectic Sm-C^*_β phase in MHPOBC was first reported as a typical ferroelectric phase [2] and later also as the phase having antiferroelectric properties [4]. We show here, that this system is a nice example of intermediate phases, which appear between main phases because of the cancellation of short range interactions and consecutive relevance of small chiral and/or longer range interactions. We present a different phenomenological model, which takes into account longer range bilinear [5] and short range biquadratic [6] interlayer interactions and allows for correct enantiomeric excess dependent phase sequence with first-order transitions between experimentally consistent structures.

Several *S*-enantiomer rich [7] mixtures of MHPOBC were studied by differential scanning calorimetry (DSC), dielectric, and optical methods. The DSC measurements were performed using Perkin Elmer DSC-7 calorimeter in the cooling and heating runs at scanning rates 0.2–1 K/min. In the dielectric measurements the glass cells of various thickness, with 25-mm^2 indium-tin oxide (ITO) electrodes coated by polimide, were used. Dielectric spectroscopy studies were performed with HP 4192A impedance analyzer. In each phase the dielectric spectra were fitted with Cole-Cole equation. The selective reflection measurements were performed in transmission mode at normal incidence (Shimadzu 3101PC spectrophotometer) for one surface free (made on the quartz plate) or film samples. These studies allowed us to determine the helical pitch in Sm-C^*_A and Sm-C^* phases. In the Sm-C^*_{FI1} and Sm-C^*_{FI2} phases the pitch was estimated by the direct microscopic observations of periodicity of the line defects in 40 μm homogeneously aligned cell. The thick (250 μm) film samples were used for the optical rotatory power (ORP) measurements, in which a standard setup was used where the analyzer is rotated against the polarizer to obtain a minimum of the light (630 nm) transmission.

In the optically pure samples (enantiomeric excess $x = c_S - c_R = \pm 1$ where c_S and c_R are corresponding concentrations) four tilted smectic subphases with historical names

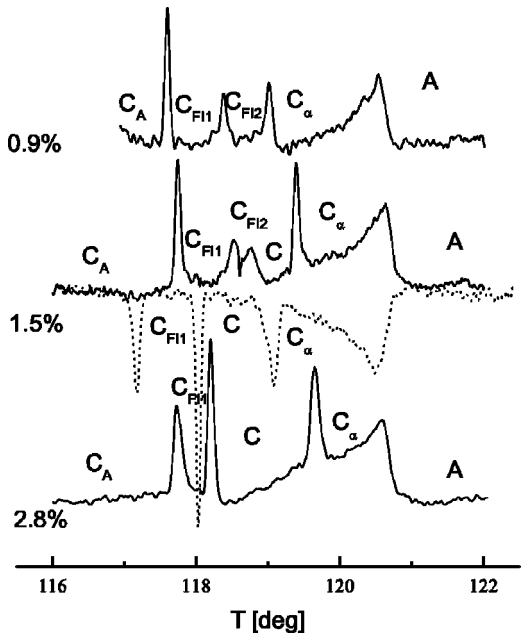

FIG. 1. DSC scans for MHPOBC mixtures with various percentage of *R* enantiomer measured in heating scans with 1-K/min rate. For concentration 1.5% the cooling scan is also shown.

Sm-C^*_α, Sm-C^*_β, Sm-C^*_γ, and Sm-C^*_A appear below the Sm-*A* phase (Fig. 1). Two phases that appear between the Sm-C^*_α and Sm-C^*_A phase, have rather long helical pitch. The periodicity of disclination lines that could be observed in the thick planar cell, is about 2.5 μm in higher temperature phase (denoted as Sm-C^*_β) and about 1.6 μm in the lower temperature phase (denoted as Sm-C^*_γ). No selective reflection in a visible range, which is encountered in the lower purity MHPOBC materials, could be detected at any temperature. Both intermediate phases have a pronounced optical activity, $+35^o/\mu$m and $-10°/\mu$m in Sm-C^*_γ and Sm-C^*_β, respectively, that is only slightly temperature dependent in the each phase temperature interval. Except for the temperature region of Sm-C^*_β, the results of ORP measurements agree with those presented in Ref. [8]. Dielectric spectroscopy measurements clearly exclude the presence of the ferroelectric synclinic Sm-*C** phase [Fig. 2(a)]. In the Sm-*A* phase, single, high frequency relaxation process is observed that softens, e.g., the mode frequency decreases and its amplitude increases, when approaching the Sm-C^*_α phase. In the Sm-C^*_α phase a single mode at $\sim$60 kHz was observed. In the Sm-C^*_β phase weak ($\Delta\varepsilon\sim4$), high frequency (350 kHz) mode was detected, typical for the phase with an antiferroelectric order. Similarly as in the Sm-C^*_A phase [9] this mode is either related to the distortion of the crystallographic unit cell or to the rotation of the molecules around their main axes. Absence of the Goldstone mode excludes that Sm-C^*_β phase is the ferroelectric Sm-*C** phase.

Dielectric permittivity increases upon entering the Sm-C^*_γ phase. Here the main contribution to the dielectric susceptibility comes from the low frequency relaxation process at 1–2 kHz, sometimes called the ferrielectric Goldstone mode [10]. The relaxation frequency of the mode detected in the

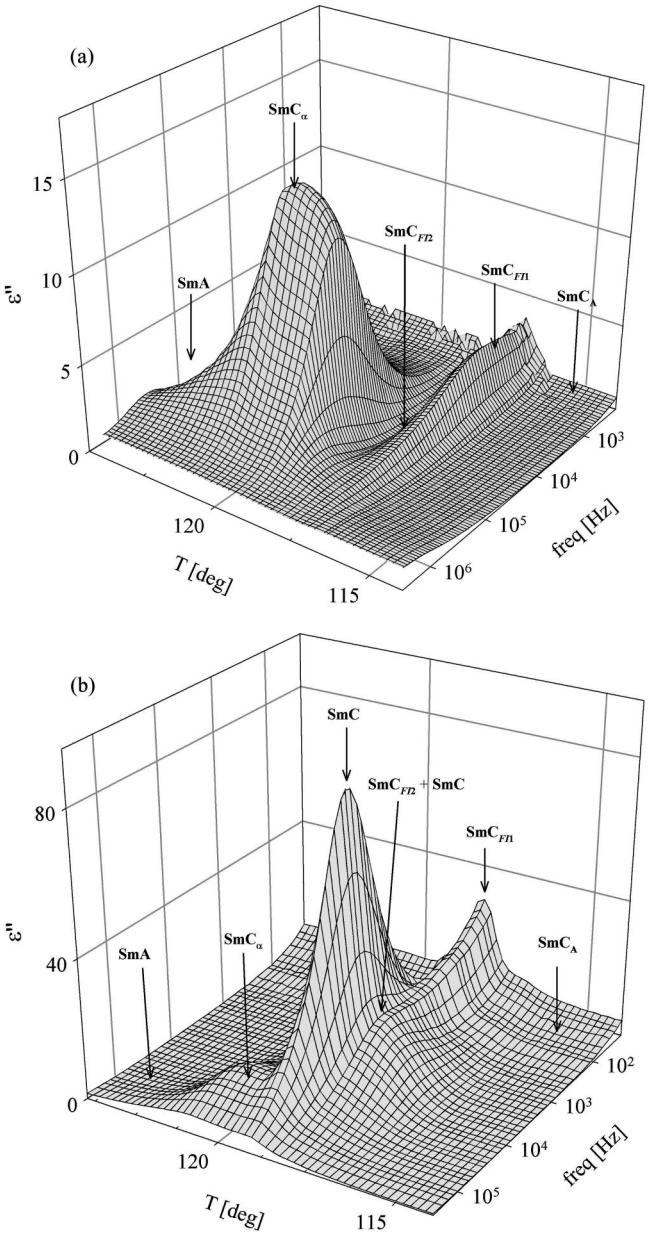

FIG. 2. Dielectric losses vs temperature and frequency in *S*-MHPOBC enantiomer (a) and its mixture with 1.5% of *R* enatiomer (b).

Sm-C^*_γ phase is not well defined. The parameter α in the Cole-Cole formula, that characterizes the distribution of the relaxation frequencies, is about 0.3. The presence of a broad mode is inherent to the Sm-C^*_γ phase. The dielectric permittivity again decreases in the Sm-C^*_A phase, in this phase two weak modes ($\Delta\varepsilon<1$) could be seen in megahertz frequency region. Above results show that the Sm-C^*_γ phase is the ferrielectric phase identical as the Sm-C^*_{FI1} and the Sm-C^*_β phase is the antiferroelectric phase, biaxial thus optically active and distinctly different than the Sm-C^*_A phase. Thus we conclude that the Sm-C^*_β phase has the distorted clock four-layer structure of the Sm-C^*_{FI2} phase.

In the samples with a slightly lower optical purity (*x*

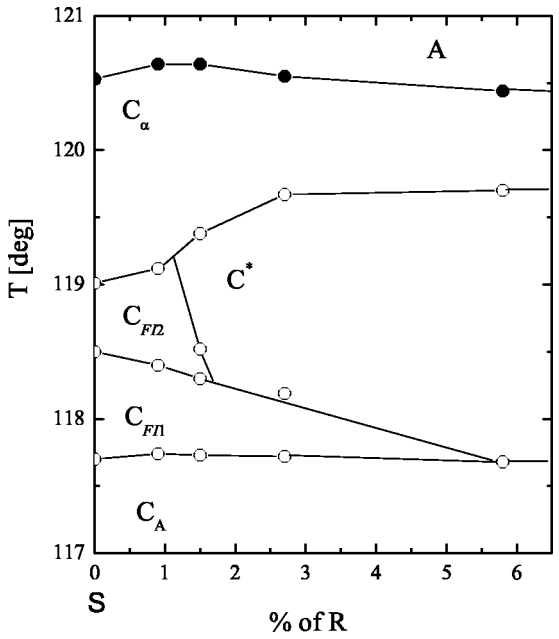

FIG. 3. Phase diagram for MHPOBC in dependence of optical purity.

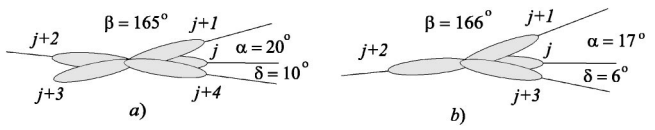

FIG. 4. (a) The Sm-C^*_{FI2} phase and (b) the Sm-C_{FI1} phase obtained for the optically pure material $x=1$ and the set of parameters expressed in K [Eq. (6), Ref. [5]]: $a_1=(-4.1+90\theta^2)$, $c_p=0.6$, $\mu=0.77$, $b_0=2$, $b_1=b_0/5$, $b_2=b_0/100$, $f_1=0$, and for $b_Q=-17.7$. Corresponding set of effective parameters expressed in mK is $\tilde{a}_2=73.5$, $\tilde{a}_3=-7.41$, $\tilde{a}_4=0.65$, $\tilde{f}_1=-231$, $\tilde{f}_2=23.1$, and $\tilde{f}_3=2.02$. The tilt angle is taken from Ref. [8] for (a) $\theta=12.5°$ and therefore $\tilde{a}_1=-69.6$ mK and for (b) $\theta=13.2°$ and $\tilde{a}_1=137$ mK.

$\sim$0.97) five subphases could be identified below Sm-*A* phase from the DSC thermograms (Fig. 1) and microscopic studies. An additional phase, which appears between the Sm-C^*_α and the Sm-C^*_{FI2} phases, gives selective reflection in the visible light range. Selective reflection wavelength changes from 450 nm to 600 nm within the phase temperature interval. Since the temperature range of the Sm-C^*_{FI2} phase in this mixture is rather narrow it is difficult to observe all five phases in the dielectric measurements. Due to the small temperature gradients that are hard to avoid in the sample with the big electrode area, the Sm-C^*_{FI2} phase always coexists with the additional phase. In this additional phase the dielectric permitivity is an order of magnitude stronger than in all other phases [Fig. 2(b)] thus typical for the synclinic ferroelectric Sm-*C** phase.

As the optical purity decreases further, the Sm-C^*_{FI2} phase disappears and in the excess range between 0.88–0.97 the phase sequence Sm-$C^*_\alpha \leftrightarrow$Sm-$C^* \leftrightarrow$Sm-$C^*_{FI1} \leftrightarrow$Sm-$C^*_A$ is observed, that is the phase sequence incorrectly reported in literature for the pure enantiomeric MHPOBC compound [2]. In mixtures with $x<0.88$ also Sm-C^*_{FI1} is missing. As the enantiomeric excess is further reduced ($x<0.5$), finally the Sm-C^*_α disappears, and only Sm-*A*, Sm-*C**, and Sm-C^*_A phases are left. Based on above observations the phase diagram in dependence on enantiomeric excess as shown in Fig. 3 is proposed. We believe that this type of the phase diagram is general for antiferroelectric liquid crystals.

To account for experimental observations theoretically, we introduce a phenomenological model with bilinear interlayer interactions between the tilt vectors $\boldsymbol{\xi}_j$ which are of longer range [5], and with biquadratic quadrupolar nearest-neighboring (NN) interactions [6], which become more important at larger tilts, i.e., at lower temperatures. The interlayer part of the free energy is

$$G_{int}=\tfrac{1}{2}\sum_j\left(\sum_{i=1}^{4}\tilde{a}_i(\xi_j\cdot\xi_{j+i})+\sum_{i=1}^{3}\tilde{f}_i(\xi_j\times\xi_{j+i})+b_Q(\xi_j\cdot\xi_{j+1})^2\right). \quad (1)$$

Achiral parameters $\tilde{a}_i$ and chiral parameters $\tilde{f}_i$ depend on steric and on van der Waals interactions NN layers, on electrostatic interactions to NN and next nearest-neighboring layers, on intralayer chiral piezoelectric, and NN flexoelectric coupling. They are given by Eq. (6) in Ref. [5]. We assume that for the racemic mixture parameter $\tilde{a}_1$ is negative favoring synclinic tilts at higher temperatures and becomes positive favoring anticlinic tilts at lower temperatures. In chiral samples it gains additional positive contribution proportional to x^2, thus changes the sign at higher temperature. Parameter $\tilde{a}_2$ is positive and does not depend on the enantiomeric excess considerably. Quadrupolar NN interactions b_Q are excess independent. All parameters are expressed in degree kelvin [5].

Numerical analysis of the above model gives the phase diagrams that are in qualitative agreement with the experimentally obtained one in Fig. 3. This detailed analysis will be published elsewhere and here only the basic physical understanding is given. In racemic mixtures the synclinic negative $\tilde{a}_1$ term prevails over the anticlinic positive $\tilde{a}_2$ term directly below the transition from the Sm-*A* to the tilted phase and the Sm-*C** phase appears. Upon decreasing temperature, $\tilde{a}_1$ increases and changes its sign at a temperature where quadrupolar term is already significant. Since this term favors both synclinic and anticlinic tilts in NN layers, direct transition from the Sm-*C** phase to the Sm-C^*_A phases is obtained. In chiral samples, the anticlinic part of the parameter $\tilde{a}_1$ increases and $\tilde{a}_1$ becomes by its absolute value comparable to the parameter $\tilde{a}_2$ directly below the transition to the tilted phase. This results in a formation of the Sm-C^*_α phase with the short pitch modulation that becomes stable over a wider temperature range upon increasing enantiomeric excess. It evolves into the Sm-*C** phase due to increasing quadrupolar interactions. Due to increased enantiomeric excess also the temperature increases where the $\tilde{a}_1$ changes sign. Therefore the influence of quadrupolar interactions is

weaker and cannot prevent the existence of modulated phases. With purification also the temperature range of modulated phases increases. In the temperature region where $\tilde{a}_1 \approx 0$ the structure with two interchanging phase differences α and β with $\alpha+\beta \approx \pi$, is formed. The quadrupolar term b_Q favors values of $\alpha=0$ and $\beta=\pi$ but chiral NN interactions increase the value of α and decrease the value of β. This structure obtained by the minimization of the Eq. (1) is consistent with a tentatively proposed structure for the Sm-C^*_{FI2} phase [11,12]. The structure has the biaxial unit cell, a negligible polarization and is helicoidally modulated with the long optical pitch defined by δ [Fig. 4(a)]. Decreasing the temperature further, the parameter $\tilde{a}_1$ becomes positive and thus simultaneously with the $\tilde{a}_3$ parameter encourages the structure where tilts in third neighboring layers are synclinic. Due to the up down symmetry, the phase difference α is followed by two equal phase differences β where $\alpha+2\beta \approx 2\pi$. The obtained unit cell is polar and biaxial. The structure is helicoidally modulated with the long optical pitch defined by δ [Fig. 4(b)]. It can be recognized as the one proposed for the Sm-C^*_{FI1} phase [11,12]. In pure samples the temperature range of the Sm-C^*_α phase and the temperature range of the modulated phases are so wide that the Sm-C^* phase cannot evolve and direct phase transition between the Sm-C^*_α phase and the Sm-C^*_{FI2} phase occurs as observed in MHPOBC.

To conclude, in this paper we report experimental and theoretical studies, which show that in the optically pure antiferroelectric liquid crystal MHPOBC, the Sm-C^*_β phase is not the ferroelectric Sm-C^* phase but the Sm-C^*_{FI2} phase with four-layer unit cell and antiferroelectric properties. The ferroelectric Sm-C^* phase appears only after a slight racemization. For antiferroelectric liquid crystals the general phase diagram with respect to enantiomeric excess is proposed. We also proposed the free energy for polar smectics that includes achiral and chiral bilinear interlayer interactions to more distant layers and quadrupolar NN interactions. This free energy allows for the correct enantiomeric excess dependent phase sequence as well as the experimentally consistent structures of all phases and first order transitions between them.

This work was supported by the Polish-Slovenian exchange program. The financial support for E.G. from Teknikvetenskapliga Forsknings Radet Swedish Research Council is acknowledged. E.G. is grateful to Professor S. Lagerwall for his hospitality during her stay at the Chalmers University.

[1] A. Fukuda, Y. Takanishi, T. Isozaki, K. Ishikawa, and H. Takezoe, J. Mater. Chem. **4**, 997 (1994).

[2] A.D.L. Chandani, E. Gorecka, Y. Ouchi, H. Takezoe, and A. Fukuda, Jpn. J. Appl. Phys., Part 2 **28**, L1265 (1989); E. Gorecka, A.D.L. Chandani, Y. Ouchi, H. Takezoe, and A. Fukuda, Jpn. J. Appl. Phys., Part 1 **29**, 131 (1990).

[3] P. Mach, R. Pindak, A.-M. Levelut, P. Barois, H.T. Nguyen, C.C. Huang, and L. Furenlid, Phys. Rev. Lett. **81**, 1015 (1998); P. Mach, R. Pindak, A.-M. Levelut, P. Barois, H.T. Nguyen, H. Baltes, M. Hird, K. Toyne, A. Seed, J.W. Goodby, C.C. Huang, and L. Furenlid, Phys. Rev. E **60**, 6793 (1999).

[4] J.F. Li, E.A. Shack, Y.K. Yu, X.Y. Wang, C. Rosenblatt, M.E. Neubert, S.S. Keats, and H. Gleeson, Jpn. J. Appl. Phys., Part 2 **35**, L1608 (1996); T. Sako, Y. Kimura, R. Hoyakawa, N. Okabe, and Y. Suzuki, *ibid.* **235**, L114 (1996); A. Jakli, J. Appl. Phys. **85**, 1101 (1999).

[5] M. Čepič and B. Žekš, Phys. Rev. Lett. **87**, 085501 (2001).

[6] D. Pociecha, E. Gorecka, M. Čepič, N. Vaupotič, B. Žekš, D. Kardas, and J. Mieczkowski, Phys. Rev. Lett. **86**, 3048 (2001).

[7] *R*- or *S*-octanol-2 with 99.5% enantiomeric excess was used for the synthesis of the MHPOBC compound as described by W.J. Drzewinski, Ph.D. thesis, Technical Miltary University, Warsaw, Poland, 2000.

[8] M. Škarabot, M. Čepič, B. Žekš, R. Blinc, G. Heppke, A.V. Kityk, and I. Muševič, Phys. Rev. E **58**, 575 (1998).

[9] Yu.P. Panarin, O. Kalinovskaya, J.K. Vij, and J.W. Goodby, Phys. Rev. E **55**, 4345 (1997).

[10] S. Merino, M.R. de la Fuente, Y. González, M.A. Pérez Jubindo, B. Ros, and J.A. Puértolas, Phys. Rev. E **54**, 5169 (1996); M. Čepič, G. Heppke, J.M. Hollidt, D. Lötzsch, and B. Žekš, Ferroelectrics **147**, 43 (1993); M. Glogarova, H. Sverenyuk, H.T. Nguyen, and C. Destrade, *ibid.* **147**, 159 (1993).

[11] T. Akizuki, K. Miyachi, Y. Takanishi, K. Ishikawa, H. Takezoe, and A. Fukuda, Jpn. J. Appl. Phys., Part 1 **38**, 4832 (1999).

[12] P.M. Johnson, D.A. Olson, S. Pankratz, T. Nguyen, J. Goodby, M. Hird, and C.C. Huang, Phys. Rev. Lett. **84**, 4870 (2000).